9TH INTERNATIONAL CONFERENCE ON COMPOSITE CONSTRUCTION IN STEEL AND CONCRETE
M. Knobloch, U. Kuhlmann, W. Kurz, M. Schäfer. (Eds.)
Stromberg, Germany, July 26-30, 2021

CHARACTERIZATION OF THE LOAD-SLIP BEHAVIOUR OF HEADED STUD SHEAR CONNECTIONS IN NARROW PROFILED SHEETING

V. Vigneri*, C. Odenbreit*, M. Schäfer*, S. Hicks, D. Lam*** and F. Hanus******

* University of Luxembourg, Faculty of Science, Technology and Medicine, Department of Engineering
e-mails: vigneri@ibk.baug.ethz.ch, christoph.odenbreit@uni.lu, markus.schaefer@uni.lu

** University of Warwick, School of Engineering
Stephen.J.Hicks@warwick.ac.uk

*** University of Bradford, Faculty of Engineering and Informatics,
Department of Civil and Structural Engineering
d.lam1@bradford.ac.uk

**** Steligence Engineering, ArcelorMittal
Francois.Hanus@arcelormittal.com

Keywords: Composite beams, Shear connectors, Headed studs, Mechanical models, Load-bearing mechanisms, Strut and tie modelling.

Abstract. *Although headed stud shear connections in profiled steel sheeting represent an efficient solution to transfer the longitudinal shear force along composite beams, the current EN 1994-1-1 may overestimate their design resistance in case of open trough profile sheeting with narrow ribs. Project team CEN/TC250/SC4.T3 proposed an alternative formula based on a "cantilever" model which depends majorly on the concrete tensile strength and the bending resistance of the stud connector. However, by increasing the slips, the internal forces redistribute, and the system can be represented by a "modified strut and tie" model. At large displacements, a "strut and tie" model was also developed accounting for the additional influence of the tensile forces in the connector. The respective analytical equations for predicting the load per stud at different slips were finally derived and compared with experimentally obtained load-slip curves. It was found that the analytical models proposed lead to satisfactory predictions of the load-slip behaviour of the shear connection.*

1 INTRODUCTION

Composite steel-concrete beams represent an optimal way to exploit the compressive strength of the concrete together with the high yield strength and ductility of structural steel. However, to ensure the composite action of steel-concrete beams, the longitudinal shear force between the concrete slab and the steel elements shall be transferred by appropriate shear connectors. In the frame of typical composite downstand beams, the most common shear connector is the headed stud which provides good structural performance in terms of strength and ductility as well as quick and easy installation. Among the different floor solutions available, two main alternatives are shown in Figure 1: the former consist of a solid slab which is typically cast-in-place whereas in the latter an additional profiled steel sheeting is employed.

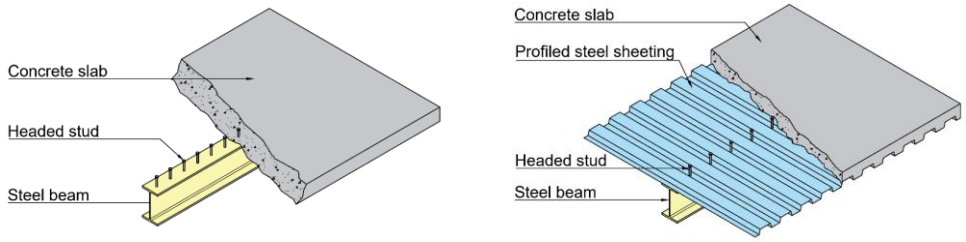

Figure 1. Typical composite steel-concrete beam with (a) solid slab and (b) transverse profiled steel sheeting

In the last decades, the construction industries have favoured the use of headed studs in combination with profiled steel sheeting transverse to the direction of the supporting beam for the use in buildings. This represents a cost-effective solution as the stud can be easily through-deck welded or placed in pre-punched holes. In parallel, the steel sheeting does not only act as formwork but it also increases the bending resistance of the slab and it reduces the concrete volume, thereby reducing the self-weight of the slab. For this purpose, several research studies were carried out alongside the appearance of more modern and sophisticated steel sheeting geometries.

The current work focuses on the analytical characterization of the entire load-slip behaviour of headed stud shear connections in modern, open trough profiled steel sheeting with narrow ribs. The motivation behind this investigation is explained in Section 2, while Section 3 provides the methodology undertaken in this contribution to achieve the objectives. The identification of three separate load bearing phases arising at different displacements is given in Section 4 and the corresponding analytical models and equations proposed are defined in Section 5. Finally, a consistent comparison between analytical predictions and experimental results is provided in Section 6 before summarizing the key outcomes and outlook for further research in Section 7.

2 MOTIVATION

Current European Standard for the design of composite constructions, namely EN 1994-1-1 [1], gives a semi-empirical formulation for determining the design strength of the connector but it does not account for the real mechanical behaviour and failure mode. This design model based on the resistance of headed studs in solid slabs including an additional reduction factor to be used with profiled sheeting was developed in the 1980-90s [2, 3, 4, 5]. It provides a sufficient level of safety for the resistance of headed studs in combination with profiled steel sheeting used at that time, which are still representing an important contribution on the market today. In the last years, the geometry of profile sheeting has indeed partially changed, some open profiled sheeting with particularly narrow ribs are available: in such cases, the distance between the headed stud and the edge of the concrete rib may be less than 60 mm at half height of the concrete rib, while no sufficient embedment depth of the headed stud above the profiled sheeting is provided or no reinforcement layer under the head of the stud is available. Those conditions are not covered by the Eurocode approach. To overcome this issue, project team CEN/TC250/SC4.T3 developed a mechanical-based approach on the basis of the push-out tests carried out within the RFCS project DISCCO [6]. However, the shear connection undergoes different stages involving the gradual damage of the concrete and the bending deformation of the connector, as already pointed out in [7] and further investigated in more recent studies [8, 9]. This work presents the analytical characterization of the load-slip behaviour of headed stud shear connections in profiled steel sheeting with narrow troughs in the frame of the research project ICO-SHEAR [10].

3 METHODOLOGY

The observation of the failure modes after testing does not generally give a clear picture of the mechanical behaviour and the resistance mechanisms activated at low displacements. Therefore, some of the experimental push-out tests carried out within this project [10] have been intentionally stopped at different slips in order to outline the progressive damage pattern of the concrete rib, as well as the bending deformation of the connector. In accordance with the objectives of the project, all the test specimens used the modern profiled steel sheeting ArcelorMittal Cofraplus 60 [11] which has particularly narrow ribs with a bottom and top width of the trough equal to 62 mm and 101 mm, respectively. Headed studs with a nominal length of 100mm and 125mm were considered in this experimental campaign using different position of the reinforcement layer.

In parallel, a validated 3D FE model was developed using the commercial software ABAQUS [12] in order to quantify the compressive stresses in the concrete and to determine the degree of activation of the plastic hinges in the stud [13]. From the evaluation of experimental evidence and the additional results from the numerical model, the mechanical response of the connection was divided into three main phases, where different load bearing mechanisms have been identified, see Figure 2. These load bearing stages and respective analytical models proposed are described in the next sections.

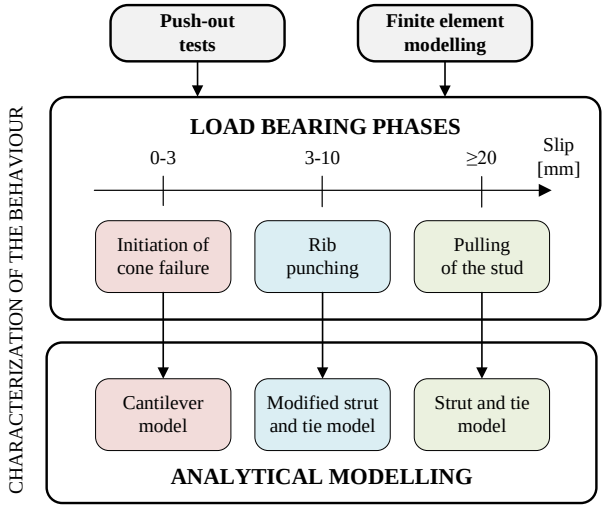

Figure 2. Methodology adopted in the present work for characterizing the load-slip behaviour of headed studs

4 LOAD BEARING PHASES

Based on the aforementioned experimental and numerical tools, three load-bearing phases in headed shear connectors employed in profiled steel sheeting were distinguished:

- Phase 1 (0-3 mm slip): Initiation of concrete cone failure (Pre-cracking stage)
- Phase 2 (3-10 mm slip): Rib punching (Post-cracking stage)
- Phase 3 (ca. 25 mm slip): Pulling of the stud (Large displacements)

4.1 Phase 1: Initiation of concrete cone failure (Pre-cracking stage)

At early stages (0-3 mm slip), the response of the shear connection is characterized majorly by the local bending deformation of the connector and the initiation of the typical concrete cone cracks. This is

confirmed by the cut section of a specimen with 100 mm long stud at a slip of ca. 2 mm given in Figure 3 where it can be observed that:

(i) Owing to the high bending stiffness of the whole concrete trough, the crack at the edge of the rib occurs at very low displacements and it starts to propagate across the rib. The crack pattern is not fully developed at this stage.

(ii) In parallel, the high bearing compressive stresses at the shank-concrete interface lead to the first diagonal crack which further propagate in the next phases.

Although no clear bending deformation can be noticed in the connector after testing, based on the supplementary numerical evaluation of the normal stresses in the stud [13], it is thought that it develops a double curvature in proximity of the weld collar.

Figure 3. Damage pattern observed after testing at a slip of ca. 2 mm [10].

4.2 Phase 2: Rib punching (Post-cracking stage)

As mentioned in the previous section, the concrete cone cracks propagate and all the internal forces redistribute accordingly. In this phase (3-10 mm slip), the force is transferred by the concrete around the stud shank which undergoes high local bearing stresses and resulting damage. To check the development of the crack path and the evolution of the damage, another specimen was likewise cut longitudinally at a slip of ca. 6 mm, as shown in Figure 4.

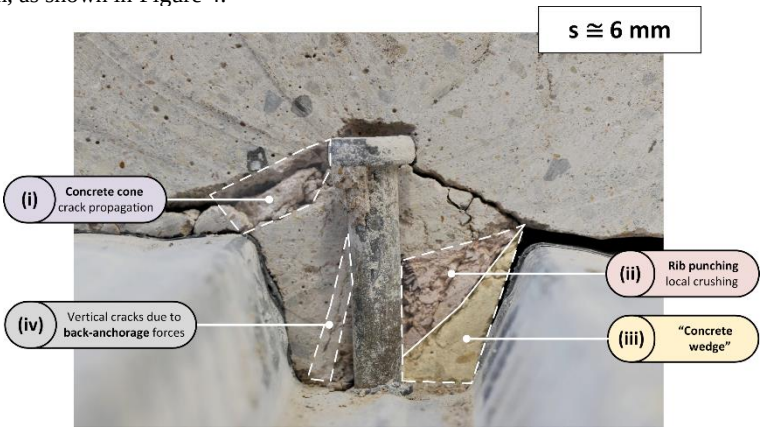

Figure 4. Damage pattern observed after testing at a slip of ca. 6 mm [10].

On that basis, the following considerations can be made:

(i) The concrete cone crack pattern spreads across the rib in a ductile manner allowing for the redistribution of the forces.

(ii) The bearing stresses acting on the stud shank increases while the damage of the concrete in front of the stud is now clearly visible: this corresponds to the so called “rib punching failure”.

(iii) As already pointed out in [14], part of the bearing forces is transferred to the steel sheeting via the "concrete wedge" which pushes against the right corner of profile.

(iv) Simultaneously, the tensile forces along the connector are balanced by the compression strut developing on the rear side of the rib, leading to the vertical crack appearing underneath the stud head.

4.3 Phase 3: Pulling of the stud (Large displacements)

By further increasing the slip, see Figure 5, a significant part of the load is carried by the connector through tension forces in this phase. The high shear and tensile stresses acting in the shank may also lead to the fracture of the stud itself.

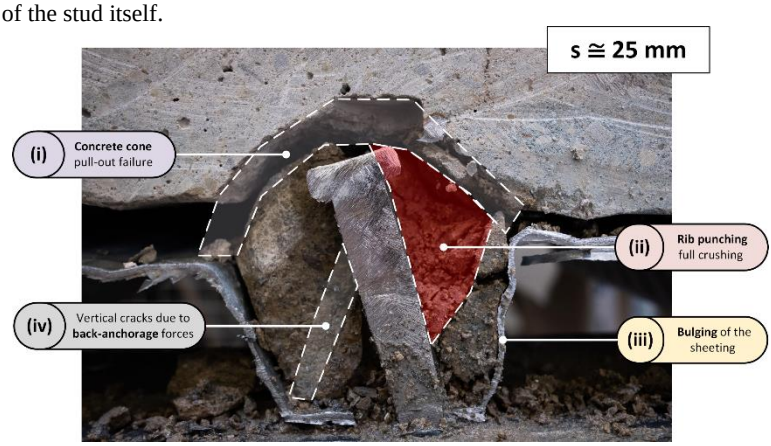

Figure 5. Damage pattern observed after testing at a slip of ca. 25 mm [10].

By analysing the longitudinal cut section of the specimen after testing (at a slip of ca. 25 mm) in Figure 5, the following considerations can be drawn:

(i) Concrete pull-out failure occurs where the cone gradually detaches from the slab due to the increasing pulling forces.

(ii) The front part of the rib is fully damaged and the bearing forces at the stud-concrete interface decrease.

(iii) The “concrete wedge” pushes further against the steel sheeting which bulges. For further displacements, the steel deck may be torn as confirmed by other studies [6].

(iv) The compressive forces acting on the rear side of the concrete rib (back-anchorage) grow further leading to the propagation of the vertical cracks.

Although the 100 mm long stud considered in this case exhibits only one plastic curvature, when longer studs are employed, it is likely that a second plastic curvature is still visible at such high displacements, as confirmed by other experimental tests [10].

5 ANALYTICAL MODELLING

The failure conditions of each model were defined in line with experimental evidences in order to determine the respective value of the load carried by the connection. These analytical values of the resistance were finally collected for the characterization of the load-slip curve of the shear connection.

For each phase identified in the previous section, a respective mechanical model was developed, respectively:

- Phase 1: Cantilever model
- Phase 2: Modified Strut and Tie model (MSTM)
- Phase 3: Strut and Tie model (STM)

Unlike Phase 1, where the concrete was modelled as a cantilever beam element (according to Euler-Bernoulli theory), the other two models considered the rib as an equivalent system of struts in accordance with the direction of the principal compressive stresses identified in the FE model. In all cases, the failure conditions of each mechanical model were consistently defined according to the experimental results and the support of further numerical studies. A detailed description of each model is given in the following subsections.

5.1 Phase 1: Cantilever model (Pre-cracking stage)

The shear connection in Phase 1 was associated to a cantilever beam model which is based on the work of Nellinger [9]. The whole connection was split in two parallel sub-systems, namely concrete cone and stud in bending, shown in Figure 6(a) and Figure 6(b) respectively.

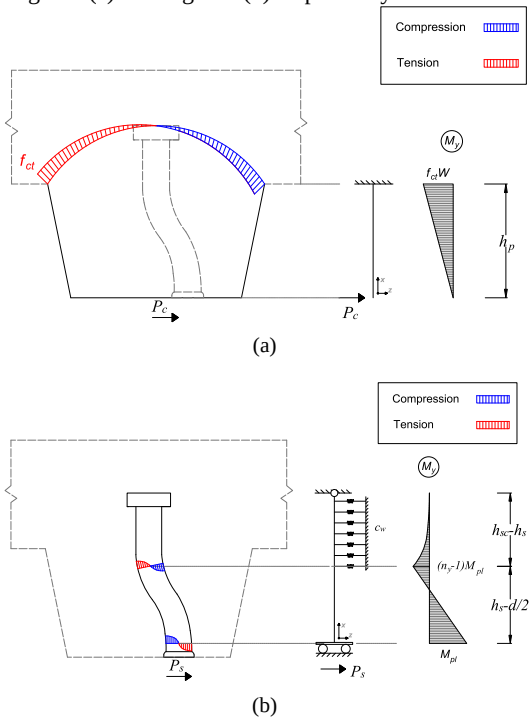

Figure 6. Cantilever model: (a) concrete cone and (b) stud in bending component [10].

It is worth noticing that the positive action of the transversal load which may apply on the slab [15] is not implicitly considered in this model although it may be implemented as an equivalent stabilizing moment preventing the rotation of the concrete rib. However, in practical applications this positive effect may not always be guaranteed due to possible counteracting lifting forces (e.g. in the zone of web openings, by continuous concrete slabs or loading directly on the steel profile), thus this effect was conservatively neglected. From the stress distribution of a linear elastic cantilever beam shown in Figure 6(a), the concrete

cone failure is assumed to initiate at the edge where the stress reaches the tensile strength of the material f_{ct}. From the rotational equilibrium equation, the respective load P_C can be easily computed as follows:

$$P_c = \frac{f_{ct} W}{n_r h_p} \tag{1}$$

And the section modulus of the concrete cone failure surface estimated in [9] is given by:

$$W = [2.4 h_{sc} + (n_r - 1) e_t] \frac{b_{max}^3}{6 b_{top}} \tag{2}$$

Where f_{ct} is the tensile strength of the concrete, n_r indicates the number of studs placed in each rib and e_t is the transversal spacing between the studs. b_{max} represents the maximum value between the widths b_{top} and b_{bot}. However, in case of open trough profiles b_{max} is always equal to b_{top}.

In parallel, the bending deformation in the connector stud induces high normal stresses. While the bending moment at the base reaches always the plastic bending resistance of the cross section (full plastic hinge), a second bending curvature may develop at a vertical coordinate h_s. As in the case of pile foundations, the degree of activation of the second plastic hinge is strongly related to the embedment provided by the surrounding concrete. Such effect was introduced in the model through a system of horizontal springs with stiffness c_w reproducing the bearing forces of the concrete, as shown in Figure 6(b). Since the value c_w can be hardly quantified analytically, the equivalent parameters n_y and h_s were used for determining the resistance component P_s. Assuming that the degree of activation of the plastic hinges n_y is known, and the bottom plastic hinge develops at a height of $d/2$ [9], the system can be solved through equilibrium equations which leads to the following value of the load P_s:

$$P_s = \frac{n_y M_{pl}}{h_s - d/2} \tag{3}$$

Where h_s and n_y can be simplified as follows:

$$h_s = 0.82 h_p \tag{4}$$

$$n_y = \begin{cases} 2 & n_r = 1 \\ 1.92 \dfrac{h_{sc} - h_p}{2d} - 2.84 \leq 2, \text{but not lower than } 1.0 & n_r = 2 \end{cases} \tag{5}$$

And:

$$M_{pl} = \frac{f_u d^3}{6} \tag{6}$$

Assuming that P_c and P_s are acting in parallel at this stage, the resulting resistance in phase 1 P_1 is given by the following expression:

$$P_1 = C \cdot k_u \left(\frac{f_{ct} W}{n_r h_p} + \frac{n_y M_{pl}}{h_s - d/2} \right) \tag{7}$$

Where the factor C was statistically estimated and defined by Eq. (8) as a function of the average width of the trough b_0. The correction factor k_u accounts for the effect of the eccentric position as well as the welding procedure and the thickness of the sheeting t, see Table 1.

$$C = 1.85 \frac{h_p}{b_0}, \quad 1.0 \leq C \leq 1.35 \tag{8}$$

Table 1: Values of the correction factor k_u.

k_u	Profiled sheeting with pre-punched holes	Through-deck welded studs	
		t <1 mm	$t \geq 1$ mm
Centred or staggered position	1.0	1.05	1.25
Favourable position	1.1	1.16	1.38
Unfavourable position	0.8	0.95	1.0

5.2 Phase 2: Modified strut and tie model (Post-cracking stage)

Unlike the strut and tie models for headed studs proposed in the past [14, 16], the "modified" strut and tie model (MSTM) proposed in this paper includes not only concrete compression struts and tension elements, but also the bending resistance component of the stud. In accordance with the numerical evaluation of the stress field in the concrete [8], the rib was replaced by a system of equivalent struts which follows the direction of the principal compressive stresses. The connector was again replaced by beam elements with two local plastic hinges. In consideration of the relatively small flexural stiffness of the profiled steel sheeting, this was assumed to transfer only tension forces, i.e. tie elements. Finally, the assembled structural system of the MSTM is illustrated in Figure 7 indicating all the main geometric variables.

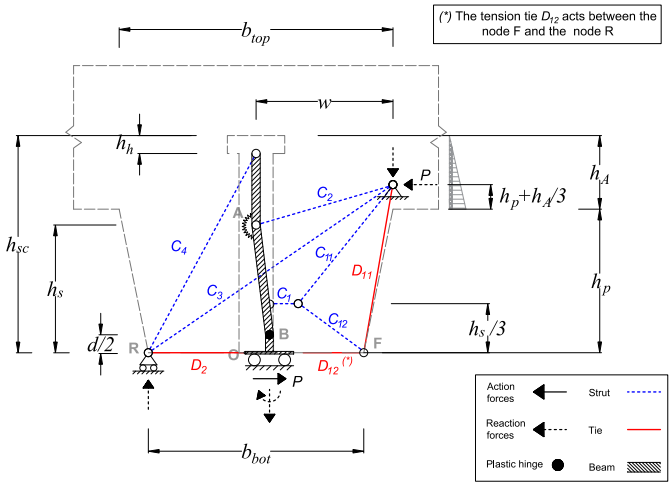

Figure 7. Modified strut and tie model [10].

Recent numerical studies on studs in profiled sheeting [17] showed the bearing forces acting at the shank of the stud are approximately linearly distributed along the segment O-A. As a result of that, the resultant force C_1 applies at a height of $h_s/3$.

As pointed out in the previous subsection, the bending moment of the stud at the base reaches the sectional plastic bending resistance while the upper hinge may partially or fully develop. Additionally, based on experimental observations, it was assumed that the sheeting locally yields and the tie element D_2 reaches its plastic resistance. Under these considerations, the system in Figure 7 is statically determined and the load P_2 can be calculated from equilibrium equations and it is given by:

$$P_2 = C_1 \cdot \zeta + \frac{n_y M_{pl}}{h_s - d/2} + D_2 \tag{9}$$

With:

$$\zeta = \frac{2h_s}{3(h_s - d/2)} \tag{10}$$

The position of the upper hinge is based on the expressions estimated by Lungershausen [7] including the influence of other parameters and it is given in Eq.(11).

$$h_s = 110\alpha_E \cdot (0.4n_r + 0.2)\left[0.8\left(\frac{n_y M_{pl}}{h_s - d/2}\right)^2 + 0.6\right][\text{mm}] \leq 1.1h_p \tag{11}$$

Assuming that the degree of activation of the plastic hinges n_y is known and the tension tie D_2 reaches its yielding capacity $D_{2,y}$, the system in Figure 7 becomes statically determined. As in the case of h_s, the value n_y was also estimated with the support of numerical simulations [13]:

$$n_y = \begin{cases} 2 & n_r = 1 \\ 1.67\,\dfrac{h_{sc} - h_p}{2d} - 0.17 \leq 2, \text{but not lower than 1.0} & n_r = 2 \end{cases} \tag{12}$$

While the capacity of the tension tie $D_{2,y}$ is equal to:

$$D_2 = D_{2,y} = k_w \cdot f_{yp}\pi d \tag{13}$$

With:

$$k_w = \begin{cases} 0.7 & \text{Pre} - \text{punched holes} \\ 1.0 & \text{Through} - \text{deck welding} \end{cases} \tag{14}$$

Where f_{yp} is the yield strength of the profiled sheeting material.

To determine the maximum resistance of this modified strut and tie model, the so called "rib punching" failure condition observed in Figure 4 was implemented. Specifically, it was supposed that the strut C_1 capacity is fully exploited considering an effective width of $2d$ and a reduced compressive strength of $0.6f_c$ in cracked concrete, as suggested by EN 1992-1-1 [18]. An analogy with the analytical modelling of RC corbels [19] was finally employed to calculate the effective depth ($k{\cdot}w$) of the strut C_1 , which was equal to the height of the section at the rib-slab interface according to linear-elastic theory applied to an equivalent corbel of depth w. Under these circumstances, the capacity of the strut $C_{1,max}$ can be written as follows:

$$C_1 = C_{1,max} = k_n \cdot (1.2f_c \cdot d \cdot k \cdot w) \tag{15}$$

With:

$$k_n = \begin{cases} 1 & n_r = 1 \\ 0.8 & n_r = 2 \end{cases} \tag{16}$$

$$k = \sqrt{x^2 + 2x} - x \tag{17}$$

Assuming the effective width of the strut equal to $2d$, x is given by:

$$x = \frac{E_s}{E_c}\frac{\pi d}{8w} \tag{18}$$

Where f_c and E_c are the compressive strength and elastic modulus of the concrete respectively while E_s is the elastic modulus of the stud material.

5.3 Phase 3: Strut and tie model (Large displacements)

Unlike the previous stages, the second-order geometric effects become predominant in this phase where the connector can transfer a significant part of the load via tensile stresses [7]. As confirmed by Figure 5, the concrete rib in front of the stud is fully damaged and thus, the corresponding bearing stresses can be neglected. The rotation of the stud head results in the gradual reduction and loss of the upper plastic hinge developed at lower displacements. Although a single plastic hinge is still activated, the analytical model representing this phase was improperly named "strut and tie" because the bending effects become comparably smaller. Since Phase 3 covers the behavior of headed stud shear connections at high displacements, the equilibrium equations may be significantly influenced by the deformation of the system. Therefore, the equilibrium equations take into account the deformed shape of the mechanical model at a slip value *s*, as shown in Figure 8.

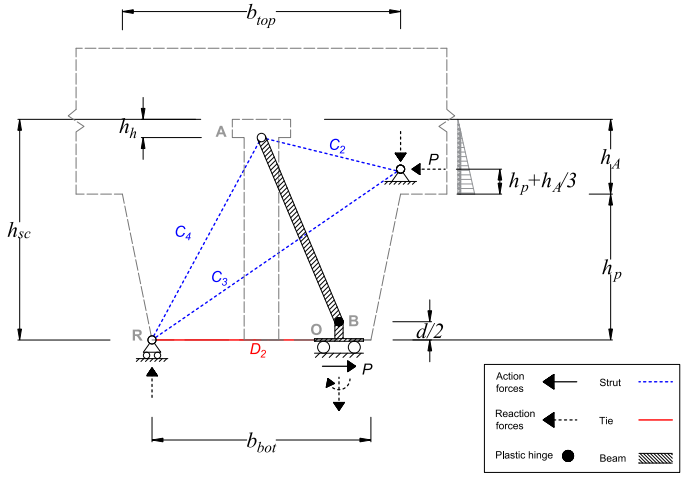

Figure 8. Strut and tie model [10].

Based on these considerations, the load P_3 can be written as:

$$P_3 = \frac{M_B \sin\phi}{(h_{sc} - h_h - d/2)^2 + s^2 - d/2} + N_B \frac{\pi d^2}{4} \cos\phi + D_2 \tag{19}$$

As done in the previous phase, it is assumed that the tension tie D_2 is yielded, i.e. $D_2 = D_{2,y}$. In consideration of the increasing tensile stress in the connector which may lead to the fracture of the shank, the bending resistance of the stud at the node B is influenced by the tensile force N_B acting on the same node. From the evaluation of the axial force at 25 mm slip extracted from FE models [10], it was found that approximately 30% of the axial capacity of the section is exploited. Hence, the maximum value of the bending moment M_B can be taken as the reduced bending resistance accounting for the *M-N* (i.e. Moment-Normal force) interaction, where the axial force N_B=0.3N_{Pl}. By using the parabolic *M-N* relationship in EN 1993-1-1 [20], the value of the bending moment M_B at failure is equal to:

$$M_B = M_{pl,N}\left(N_B = 0.3N_{pl}\right) = 0.91M_{pl} \tag{20}$$

6 COMPARISON BETWEEN ANALYTICAL AND EXPERIMENTAL RESULTS

The analytically-computed load values obtained from Equations (7), (9) and (19) for phase 1, 2 and 3 respectively, can be gathered to extract an analytical load-slip relationship which was finally compared

with the experimental results in this section. In order to have a consistent comparison between the experimental and analytical prediction of the load-slip curve, the corresponding experimental values P_{e1}, $P_{e,2}$ and $P_{e,3}$ were calculated as the maximum load value within the slip range of each phase, see Figure 9. A good agreement between test and analytical load-slip curves was reached, as confirmed by Figure 10, especially at low displacements, i.e. in phase 1 and 2. On the other hand, the strut and tie model of Phase 3 provides a conservative estimation of the respective load at high displacements which may be due to the fact that the resistance of the concrete was completely neglected at this stage. Owing to the nature of the load-slip behaviour of the shear connector in the first slip displacements, it can be said that both "cantilever model" and modified strut and tie model (MSTM) can be used to determine appropriately the load bearing capacity of these shear connections.

These outcomes confirm the suitability of the "MSTM" and, more importantly, the "cantilever model" for studs in sheeting with narrow troughs. The latter was included in the design proposal of the revised version of EN 1994-1-1 presented by project team CEN/TC250/SC4.PT3 to cover cases with relatively slender rib geometries and it is currently under consideration.

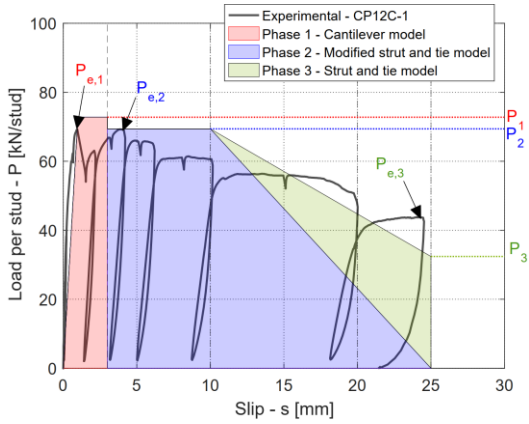

Figure 9. Example of experimental and analytical load-slip curve [10].

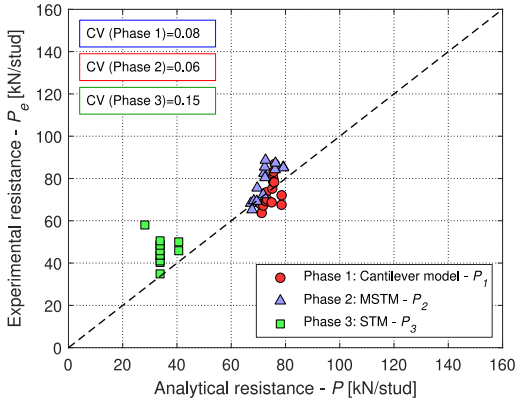

Figure 10. Comparison between experimental and analytically calculated value of the load in each phase for the push-out tests with narrow profiled steel sheeting [10].

7 SUMMARY AND OUTLOOK

The sequence of different load bearing mechanisms in headed stud shear connections employed in profiled steel sheeting with narrow troughs was identified through experimental tests and numerical studies on push-out test specimens. Three load-bearing phases were distinguished at different slip displacements and the corresponding mechanical models were developed for predicting the load-slip behaviour of the connection. The suitability of the models presented was finally confirmed by the good agreement with experimentally obtained load-slip curves. It was also seen that the cantilever model (Phase 1) and modified strut and tie model (Phase 2) are suitable for predicting the maximum load carried by the shear connector.

However, a wider push-test database may be considered in the future to assess the reliability as well as the scope of application of such analytical equations enabling the calibration of design proposals.

REFERENCES

[1] British Standards Institution, "EN 1994-1-1:2004 Eurocode 4 - Design of composite steel and concrete structures Part 1-1: General rules and rules for buildings," London, 2004.

[2] K. Roik and G. Hanswille, "Tragfähigkeit von Kopfbolzendübeln, Hintergrundbericht zu Eurocode 4.," Bericht EC4/12/89, 1989.

[3] H. Bode and R. Künzel, "Zur Verwendung von Profilblechen beim Trägerverbund," *Der Metallbau im Konstruktiven Ingenieurbau,* vol. Festschrift Rolf Baehre, 1990.

[4] R. P. Johnson and H. Dongjie, "Resistance to longitudinal shear of composite beams with profiled sheeting," *Proceedings of the Institution of Civil Engineers-Structures and Buildings,* vol. 110, no. 2, pp. 204-215, 1995.

[5] G. Hanswille, C. Kajzar and A. Faßbender, "Ergänzende Regelungen für die Tragfähigkeit von Kopfbolzendübeln bei Verwendung von vorgelochten Profilblechen," Forschungsbericht 93-01, Wuppertal, 1993.

[6] M. Lawson, E. Aggelopoulos, R. Obiala, F. Hanus, C. Odenbreit, S. Nellinger, U. Kuhlmann, F. Eggert, D. Lam, X. Dai and T. Sheehan, "Development of improved shear connection rules in composite beams - Final Report," 2017.

[7] Lungershausen, "Zur Schubtragfähigkeit von Kopfbolzendübeln. Ph.D. Dissertation," Ruhr universität bochum, 1988.

[8] V. Vigneri, C. Odenbreit and D. Lam, "Different load bearing mechanisms in headed stud shear connectors for composite beams with profiled steel sheeting," *Steel Construction,* vol. 12, no. 3, pp. 184-190, 2019.

[9] S. Nellinger, "On the behaviour of shear stud connections in composite beams with deep decking. Ph.D. Dissertation," Luxembourg, 2015.

[10] V. Vigneri, "Load bearing mechanisms of headed stud shear connections in profiled steel sheeting transverse to the beam. Ph.D. Dissertation," University of Luexmbourg, Luxembourg, 2021.

[11] ArcelorMittal-Construction, "Technical datasheet Cofraplus® 60 - Composite floor decking," ArcelorMittal, 2015. [Online]. Available: https://construction.arcelormittal.com/..

[12] Dassault Systèmes Simulia, "Abaqus Analysis User's Guide v6.14," 2014.

[13] V. Vigneri, C. Odenbreit and M. V. Braun, “Numerical evaluation of the plastic hinges developed in headed stud shear connectors in composite beams with profiled steel sheeting,” *Structures,* vol. 21, pp. 103-110, 2019.

[14] S. Ernst, “Factors Affecting the Behaviour of the Shear Connection of Steel-Concrete Composite Beams. Ph.D. Dissertation,” University of Western Sydney, Sydney, 2006.

[15] S. Nellinger, C. Odenbreit, R. Obiala and M. Lawson, “Influence of transverse loading onto push-out tests with deep steel decking,” *Journal of Constructional Steel Research,* vol. 128, pp. 335-353, 2017.

[16] R. P. Johnson and H. Yuan, “Existing rules and new tests for stud,” *Proceedings of the Institution of Civil Engineers - Structures and Buildings,* vol. 128, no. 3, pp. 244-251, 1998.

[17] M. Shen, “Structural behaviour of shear connection in composite structures under complex loading conditions. Ph.D. Dissertation,” Hong Kong, 2014.

[18] British Standards Institution, “EN 1992-1-1:2004 Eurocode 2 - Design of concrete structures Part 1-1: General rules and rules for buildings,” 2004.

[19] S. Hwang, W. Lu and H. Lee, “Shear Strength Prediction for Reinforced Concrete Corbels,” *ACI Structural Journal* , vol. 97, no. 4, p. 543–552., 2000.

[20] British Institution Institute, “EN 1993-1-1:2004 Eurocode 3 - Design of steel structures Part 1-1: General rules and rules for buildings,” 2004.